

AD-A232 082

NASA Contractor Report 187483

ICASE Report No. 90-87

# ICASE

ASYMPTOTIC-INDUCED NUMERICAL METHODS  
FOR CONSERVATION LAWS

Marc Garbey  
Jeffrey S. Scroggs

Contract No. NAS1-18605  
December 1990

Institute for Computer Applications in Science and Engineering  
NASA Langley Research Center  
Hampton, Virginia 23665-5225

Operated by the Universities Space Research Association

National Aeronautics and  
Space Administration

Langley Research Center  
Hampton, Virginia 23665-5225

**DISTRIBUTION STATEMENT A**

Approved for public release;  
Distribution Unlimited

DTIC  
ELECTE  
FEB 22 1991  
S B D

91 2 19 124

# ASYMPTOTIC-INDUCED NUMERICAL METHODS FOR CONSERVATION LAWS

Marc Garbey  
University Claude Bernard Lyon1  
LAN, 69622 Villeurbanne cedex  
France

and

Jeffrey S. Scroggs<sup>1</sup>  
Institute for Computer Applications in Science and Engineering  
NASA Langley Research Center  
Hampton, VA 23665

## ABSTRACT

Asymptotic-induced methods are presented for the numerical solution of hyperbolic conservation laws with or without viscosity. The methods consist of multiple stages. The first stage is to obtain a first approximation by using a first-order method, such as the Godunov scheme. Subsequent stages of the method involve solving internal-layer problems identified by using techniques derived via asymptotics. Finally, a residual correction increases the accuracy of the scheme. The method is derived and justified with singular perturbation techniques.

---

<sup>1</sup>This research was supported by the National Aeronautics and Space Administration under NASA Contract No. NAS1-18605 while the author was at the Institute for Computer Applications in Science and Engineering (ICASE), NASA Langley Research Center, Hampton, Virginia 23665. This work was also supported by the Applied Mathematical Sciences subprogram of the Office of Energy Research, U. S. Department of Energy, under Contract W-31-109-Eng-38 and DRET.

# 1 Introduction

The combination of asymptotic and numerical analyses provides improved accuracy for multiple-scales problems<sup>2</sup>. Many physical problems have multiple scales; a typical situation occurs when physics on the fastest scale induces narrow regions where the variation in the solution is large. Such regions are called *boundary layers* or *transition layers*, depending on whether they are near a boundary or inside the interior of the domain. Examples of such situations are laminar flow of a slightly viscous fluid or combustion with high activation energy. Classical schemes applied to these types of situation generally fail to correctly describe the behavior inside the layers. This difficulty is overcome by developing numerical methods based on the asymptotic analysis of the multiple-scales problems. We demonstrate how asymptotic analysis and numerical analysis can interact to achieve the goal of a highly accurate solution method.

The numerical techniques developed in this paper are designed to solve two problems: hyperbolic conservation problems with or without viscosity. Also, we treat three different types of singularity arising in inviscid and viscous conservation laws, using domain decomposition: specifically, we solve problems that have *shocks*, *weak singularities*, and *interaction of singularities*. We use an asymptotic analysis to identify the appropriate scalings as well as modified problems in the transition layers. The domain decomposition of our numerical method is then based on the criterion given by the asymptotic analysis. The numerical algorithms involve several stages to solve each modified problem in the layers. Finally, we treat weak singularities with a residual correction. The residual correction also identifies incorrect asymptotic preconditioning and controls the numerical accuracy of the solution.

A number of recent papers present new numerical methods that are induced by an asymptotic analysis. For example, basis functions motivated by asymptotics of boundary layers are developed in [3]. Many of the basic ideas relating to asymptotic analysis and numerical methods that use domain decomposition are found in [2]. These ideas were incorporated into a parallel numerical method in [15]. Specific applications to problems involving conservation laws have been developed in [1].


On the other hand, some recent papers used the singular perturbation approach to investigate the effect of viscosity on conservation laws. Sharp estimates can be found, for example, in [10] and its references. The dynamics of internal layers are studied in [6]. Also, uniform approximation based on the matching asymptotic technique are given in [8] and [7].

This paper is a further stage toward the synthesis of asymptotic analysis and numerical methods applied to systems of viscous conservation laws (seen as a singular perturbation problem). We begin with an asymptotic analysis of the problem in Section 2. This analysis is expanded and combined with numerical techniques in Section 3. We end with a demonstration of the techniques on computational fluid dynamics problems in Section 4.

## 2 Asymptotic Analysis

In this section we present the problem and briefly review the asymptotic analysis that is used in the method. The result is a uniform approximation based on the asymptotic technique of

<sup>2</sup>In this manuscript we shall solve all important problems of current interest, except possibly inflation.



<input checked="" type="checkbox"/>	
<input type="checkbox"/>	
<input type="checkbox"/>	
y Codes	
and/or	
Special	

A-1

matching [5].

Asymptotic analysis that is strongly coupled with the numerical analysis is delayed until later in the paper.

## 2.1 Setting of the Problem and Regular Expansion

Consider the Cauchy problem

$$\begin{cases} \frac{\partial U}{\partial t} + \frac{\partial}{\partial x} F(U) = \epsilon \frac{\partial}{\partial x} \left( P(U) \frac{\partial U}{\partial x} \right) & \text{for } (x, t) \in \Omega \\ U(x, 0) = V(x) & \text{for } x \in \mathbb{R}. \end{cases} \quad (1)$$

Here the solution  $U : \Omega \rightarrow \mathbb{R}^n$  is a vector-valued function, the domain is  $\Omega = \mathbb{R} \times ]0, T[$ , and  $\epsilon \ll 1$  is a small parameter.

We assume that  $V$  is piecewise smooth. We also assume that  $F$  and  $P$  are smooth functions of  $U$ . We suppose that  $P$  is a *suitable viscosity matrix* [4] for the shocks of the following associated inviscid problem:

$$\begin{cases} \frac{\partial U}{\partial t} + \frac{\partial}{\partial x} F(U) = 0 & \text{for } (x, t) \in \Omega \\ U(x, 0) = V(x) & \text{for } x \in \mathbb{R}. \end{cases} \quad (2)$$

That is, a shock wave solution to (2) can be obtained as a limit of progressive wave solutions of (1). Problem (1) is a parabolic-hyperbolic singular perturbation problem driven by (2).

One easily obtains the regular expansion

$$U_{\text{reg}}^{\text{outer}} = U^0 + \epsilon U^1 + \epsilon^2 U^2 + \dots \quad (3)$$

that is *a priori* valid outside the neighborhood of the singularities of the solution to (2). We substitute  $U_{\text{reg}}^{\text{outer}}$  in the differential equation of (1) and use identification in  $\epsilon$  to obtain that  $U^0$  must be a solution of (2). We also find that  $U^1$  must be a solution of the following linear hyperbolic problem:

$$\begin{cases} \frac{\partial U^1}{\partial t} + \frac{\partial}{\partial x} (DF(U^0)U^1) = \frac{\partial}{\partial x} \left( P(U^0) \frac{\partial U^0}{\partial x} \right) & \text{for } (x, t) \in \Omega \\ U^1(x, 0) = 0 & \text{for } x \in \mathbb{R}, \end{cases} \quad (4)$$

where  $DF$  denotes the Jacobian matrix of  $F$ . In general, the equation for the term  $U^i$  with coefficient  $\epsilon^i$  is the solution to the analogous differential equation

$$\frac{\partial U^i}{\partial t} + \frac{\partial}{\partial x} (DF(U^0)U^i) = RHS(U^j, j < i),$$

with a right-hand side that depends on the previous terms. The inviscid problem (2) has many weak solutions; we shall uniquely define  $U^0$  as the analysis progresses.

It is most common to complete  $U_{\text{reg}}^{\text{outer}}$  with a  $U_{\text{reg}}^{\text{inner}}$  for each singular region to obtain a uniformly valid approximation to a viscous problem. However, we shall develop in detail only

the asymptotic analysis that is required for our numerical methods. Thus we restrict our asymptotic analysis to complete  $U_{\text{aa}}^{\text{outer}}$  with  $U_{\text{aa}}^{\text{inner}}$  only when the singularity is a shock layer. The solution is completed for weak singularities with the residual correction techniques of Section 3.4. This completion also results in a uniformly valid approximation. Furthermore, the approximation is not difficult to obtain numerically. It is easy to see that interaction of singularities requires a stretching in both the space and time variables: this leads to some parabolic layers. We shall use a numerical treatment of the interaction of singularities that does not require a complete analysis of these parabolic layers.

## 2.2 Transition Layer That Corresponds to Shock Waves

We assume that solutions  $U^0$  of (2) are smooth except on piecewise regular curves  $S_k(t)$ . It is assumed for  $t \in [t_0, t_1]$  that the  $S_k$  are isolated from each other. Without loss of generality we may drop the subscript  $k$ .  $S$  is assumed to be smooth for  $t \in [t_0, t_1]$ . In particular, we assume no focusing of characteristics. To make this more precise, we suppose that there is an interval of time  $[t_0, t_1]$  such that for each  $t \in [t_0, t_1]$  and for each  $S$  the following limits exist:

$$U_l^0 = \lim_{x \rightarrow S^-(t)} U^0(x, t), \quad U_r^0 = \lim_{x \rightarrow S^+(t)} U^0(x, t),$$

Let us define the change of variable:  $\tilde{x} = x - S'(t)t$  and  $\tau = t$ . We denote  $\tilde{U}(\tilde{x}, \tau) = U(x, t)$ . We further assume that

$$\begin{aligned} U_{\tau, l}^0 &= \lim_{\tilde{x} \rightarrow 0^-} \frac{\partial U^0}{\partial \tau}, & U_{\tau, r}^0 &= \lim_{\tilde{x} \rightarrow 0^+} \frac{\partial U^0}{\partial \tau}, \\ U_{j, l}^i &= \lim_{\tilde{x} \rightarrow 0^-} \frac{\partial^i U^j}{\partial \tilde{x}^i}, & U_{j, r}^i &= \lim_{\tilde{x} \rightarrow 0^+} \frac{\partial^i U^j}{\partial \tilde{x}^i}, \quad \text{for } i, j \geq 0, \\ U_{\tau, l}^0 &= O(1), & U_{\tau, r}^0 &= O(1). \end{aligned}$$

The shock layer profile will not have rapid variation, so it is appropriate to scale and translate only the spatial variable (and not the temporal variable). Such a transformation is defined by

$$\xi = \frac{x - S(t)}{\epsilon} \quad \text{and} \quad \tau = t, \quad (5)$$

where we denote  $\hat{U}(\xi, \tau) = U(x, t)$ . Under this transformation the differential equation of problem (1) becomes

$$\frac{\partial \hat{U}}{\partial \tau} + \epsilon^{-1} \frac{\partial}{\partial \xi} (F(\hat{U}) - S(\tau)\hat{U}) = \epsilon^{-1} \frac{\partial}{\partial \xi} \left( P(\hat{U}) \frac{\partial \hat{U}}{\partial \xi} \right). \quad (6)$$

This suggests an inner expansion of the form

$$\hat{U}_{\text{aa}}^{\text{inner}} = \hat{U}^0 + \epsilon \hat{U}^1 + \epsilon^2 \hat{U}^2 + \dots, \quad (7)$$

where all of the terms  $\hat{U}^i$  are functions of  $\xi$  and  $\tau$ . Using this expansion in (6) and imposing the matching relations [5, 8] with the outer expansion  $U_{\text{aa}}^{\text{outer}}$ , we derive the set of ODE

problems for the  $\hat{U}^i$ . The equation for the first term is

$$\begin{cases} -\frac{\partial}{\partial \xi} \left( P(\hat{U}^0) \frac{\partial \hat{U}^0}{\partial \xi} \right) + \frac{\partial}{\partial \xi} \left( F(\hat{U}^0) - S'(t)\hat{U}^0 \right) = 0, \\ \hat{U}^0 \rightarrow U_l^0 \text{ as } \xi \rightarrow -\infty \\ \hat{U}^0 \rightarrow U_r^0 \text{ as } \xi \rightarrow +\infty \end{cases} \quad (8)$$

and for the second term we have

$$\begin{cases} -\frac{\partial^2}{\partial \xi^2} \left( P(\hat{U}^0) \cdot \hat{U}^1 \right) + \frac{\partial}{\partial \xi} \left( DF(\hat{U}^0) \cdot \hat{U}^1 - S'(t)\hat{U}^1 \right) = -\frac{\partial \hat{U}^0}{\partial \tau}, \\ \|\hat{U}^1 - (U_{0,l}^1 \xi + U_{1,l}^0)\|_o \rightarrow 0 \text{ as } \xi \rightarrow -\infty \\ \|\hat{U}^1 - (U_{0,r}^1 \xi + U_{1,r}^0)\|_o \rightarrow 0 \text{ as } \xi \rightarrow +\infty, \end{cases} \quad (9)$$

where  $\|U\|_o = \max_{i=1..n}(|u_i|)$  for  $U = (u_i)_{i=1..n}$ . More generally, we obtain

$$\begin{cases} -\frac{\partial^2}{\partial \xi^2} \left( P(\hat{U}^0) \cdot \hat{U}^i \right) + \frac{\partial}{\partial \xi} \left( DF(\hat{U}^0) \cdot \hat{U}^i - S'(t)\hat{U}^i \right) = RHS_i(\hat{U}^j, j < i), \\ \|\hat{U}^0 - \sum_{j=0}^i \frac{1}{(i-j)!} U_{j,l}^{i-j} \xi^{i-j}\|_o \rightarrow 0 \text{ as } \xi \rightarrow -\infty \\ \|\hat{U}^0 - \sum_{j=0}^i \frac{1}{(i-j)!} U_{j,r}^{i-j} \xi^{i-j}\|_o \rightarrow 0 \text{ as } \xi \rightarrow +\infty \end{cases} \quad (10)$$

where the right-hand side is a nonlinear function depending on the  $\hat{U}^j$  for  $j < i$ . Identification of the coefficients of the appropriate power of  $\epsilon$  in the differential equation of problem (6) determines  $RHS_i$ .

The temporal variable  $\tau$  can be considered as a parameter in the transition layer because the above problems require the solution of only ODEs. Also, the problems for  $\hat{U}^i$  are linear for  $i > 0$ . Being able to treat  $\tau$  as a parameter is not surprising, since  $U_{\tau,l}^0 = O(1)$  and  $U_{\tau,r}^0 = O(1)$ .

Next we discuss the existence of  $\hat{U}_0$  and the uniqueness of  $U_0$  as well as the uniqueness of the curve  $S$ . Using a matching relation on the first spatial derivatives on the terms in the expansion  $U_{\text{as}}^{\text{inner}}$ , one looks for  $\hat{U}^0$  such that

$$\frac{\partial \hat{U}^0}{\partial \xi} \rightarrow 0 \text{ as } \xi \rightarrow \pm\infty.$$

We integrate (8) from  $-\infty$  to  $\xi$  to obtain

$$P(\hat{U}^0) \frac{\partial \hat{U}^0}{\partial \xi} = H(\hat{U}^0) - H(U_l^0), \quad (11)$$

where  $H(U) = F(U) - S'(t)U$ . Thus, the existence of a solution to (8) implies the Rankine and Hugoniot condition (RH)

$$H(U_l^0) = H(U_r^0).$$

This means that  $U_l^0$  and  $U_r^0$  are critical points of the dynamical system (11).

In addition to the RH condition, we must be able to construct the layer; thus, we assume

There exists a unique trajectory for the  
 dynamical system (11) from  $U_l^0$  to  $U_r^0$ .

H1.

It is interesting to compare H1 with the classical geometric entropy condition (GEC). For scalar conservation laws, H1 is equivalent to the GEC [11] [14]; however, this is not in general true. A number of very interesting studies have considered which conditions one can expect that the GEC implies H1. In particular, the GEC implies H1 when  $P$  is the identity and the problem consists of a  $2 \times 2$  system with the assumption of genuine nonlinearity [4, 12]. The existence of a viscous profile (i.e., H1) is not of the same nature as the GEC. However, we restrict our problems to cases where the RH condition and H1 are enough to uniquely define  $U^0$  and  $S$  (and consequently  $U_{aa}^{\text{outer}}$ ).

Now we have determined  $\hat{U}^0$  up to a translation in the spatial variable  $\xi$ . In Section 2.2 this translation will be imposed as a solvability condition on the solutions to problem (9).

### 2.3 Construction of the Inner Expansion in the Shock Layer

Here we briefly outline the construction of the solution in the shock layer. This formal theory for systems of conservation laws is a generalization of the construction in the case of scalar conservation laws [8]. For more details of this generalization, see [9].

Let us concentrate on the construction of the solution  $\hat{U}^1$  of problem (9). The procedure is first to obtain two functions  $\hat{U}_l^1(\xi, t)$  and  $\hat{U}_r^1(\xi, t)$  as solutions to related problems, then combine them such that the resulting function is a smooth solution of (9). The function  $\hat{U}_l^1$  satisfies the equation from problem (9) with the left boundary condition

$$\hat{U}^1 - (U_{0,l}^1 \xi + U_{1,l}^0) \rightarrow 0 \quad \text{as } \xi \rightarrow -\infty,$$

whereas  $\hat{U}_r^1$  satisfies the equation from problem (9) with the right boundary condition

$$\hat{U}^1 - (U_{0,r}^1 \xi + U_{1,r}^0) \rightarrow 0 \quad \text{as } \xi \rightarrow +\infty.$$

We use the solutions to these problems that are constructed using an element  $\partial \hat{U}^0 / \partial \xi$ , of the kernel of (9). That is, we construct  $\hat{U}^1$  as the function

$$\hat{U}^1(\xi, t) = \begin{cases} \hat{U}_l^1(\xi, t) + B_l(t) \times \frac{\partial \hat{U}^0}{\partial \xi} & \text{for } \xi \leq 0 \\ \hat{U}_r^1(\xi, t) + B_r(t) \times \frac{\partial \hat{U}^0}{\partial \xi} & \text{for } \xi \geq 0, \end{cases}$$

where  $U \times V$  denotes the vector  $(u_i v_i)_{i=1..n}$ .  $B_l$  and  $B_r$  are some smooth vector functions from  $\Omega$  into  $\mathbb{R}$  that satisfy the continuity condition

$$\hat{U}_l^1(0, t) + B_l(t) \times \frac{\partial \hat{U}^0}{\partial \xi}(0, t) = \hat{U}_r^1(0, t) + B_r(t) \times \frac{\partial \hat{U}^0}{\partial \xi}(0, t).$$

Notice that for a fixed value of  $t$ , this relation determines the vector functions up to a single constant.

One can prove [9] that  $\hat{U}^1$  is a smooth function iff  $\hat{U}^0$  satisfies the relation

$$\begin{aligned} \frac{\partial}{\partial t} \left\{ \int_{-\infty}^0 (\hat{U}^0(\xi, t) - U_l^0(t)) d\xi + \int_0^{\infty} (\hat{U}^0(\xi, t) - U_r^0(t)) d\xi \right\} \\ = \left\| \left[ S'(t)U^1 - DF(U^0) \cdot U^1 + P(U^0) \frac{\partial U^0}{\partial x} \right] \right\|, \end{aligned}$$

where  $[\cdot]$  denotes the jump across the shock. This is simply an area relation that determines the shift in  $\xi$  for  $\hat{U}^0$ . Let us assume for simplicity that  $U$  and its space derivatives vanish at infinity. One can show that this relation is a consequence of the conservation relation

$$\int_{-\infty}^{\infty} \frac{\partial U}{\partial t} = 0,$$

satisfied by solutions to (1) and (2). This relation is also satisfied by our uniform approximation of the solution to (1), where

$$U_{as} = (1 - H(\xi_\nu))U_{as}^{outer} + H(\xi_\nu)(\hat{U}^0 + \epsilon\hat{U}^1) + O(\epsilon^2).$$

Here  $\xi_\nu = (x - S(t))/\epsilon^\nu$  is the intermediate variable and  $H$  is a smooth cutoff function

$$H(y) = \begin{cases} 0 & \text{if } |y| > 2 \\ 1 & \text{if } |y| < 1. \end{cases}$$

More precisely, we have

$$\int_{-\infty}^{\infty} \frac{\partial U_{as}}{\partial t} = O(\epsilon),$$

We currently have defined  $\hat{U}^1$  up to a kernel function of (9). Since we use only the first term  $\hat{U}^0$  in the current implementation of this method, we do not discuss how to determine this constant here. This construction can be pursued at any order. For example, the solvability condition for problem (10) with  $i = 2$  will select the only admissible  $\hat{U}^1$  solution of problem (9) [8].

### 3 Asymptotic-Induced Numerical Scheme

Now we consider the numerical treatment of problems (1) and (2) by using the analysis in the previous sections.

#### 3.1 Localization of the Singularities

Let  $\{x_i\}_{i=\dots,-1,0,1,\dots}$  be the spatial discretization of step size  $\Delta x$ , and let  $\{t_k\}_{k=1,\dots}$  be the temporal discretization of step size  $\Delta t$ . For convenience we restrict the discussion on localization of singularities to scalar conservation laws. The scalar terms are distinguished from the system by using the notation  $u$  and  $f$  as the solution and flux function in place of  $U$  and  $F$ , respectively. We suppose that  $u$  is known at time  $t_k$ . Starting from  $u(\cdot, t_k)$ , we apply a



Table 1: Asymptotic Order of Residual

Type of Zone	Order of Residual $u_t + f(u)_x$	Local Coordinates	
		$\xi$	$\tau$
Regular zone	$O(\epsilon)$	$x$	$t$
Shock layer	$O(\epsilon^{-1})$	$(x - S(t))/\epsilon$	$t$
Weak singularity	$O(\epsilon^{1/2})$	$(x - S(t))/\epsilon^{1/2}$	$t$
Shock interaction with other singularities	$O(\epsilon^{-1})$	$(x - S_0 - S_1 t)/\epsilon$	$(t - t_0)/\epsilon$
Discontinuous with $f$ locally linear	$O(1)$	$(x - S_0 - S_1 t)/\epsilon^{1/2}$	$t - t_0$
Formation of shock	$O(\epsilon^{-1/4})$	$(x - S_0 - S_1 t)/\epsilon^{3/4}$	$(t - t_0)/\epsilon^{3/4}$

discretization that gives an approximation  $\tilde{u}^K$  at the discrete spatial points  $\{x_i\}$  at time  $t_K$ , where  $K > k$ . Given this approximation, we discuss the problem of localization of different types of singularities of  $u$  at time  $t_K$ .

Localizing the singularities will use the residual obtained from the left-hand side of the PDE in (1). To this end, we recall in Table 1 some results of the asymptotic analysis of the Cauchy problem (1); see [8] and its references. Here  $S_0$  and  $S_1$  are the constants from the local linearization  $S(t) = S_0 + S_1 t + O((t - t_0)^2)$  in the neighborhood of the singularity.

The localization is presented for the case when  $\tilde{u}^K$  is obtained by using the first-order Godunov scheme; however, this analysis requires only minor modification for several first-order discretizations of scalar conservation laws, provided the discretizations are conservative. The solution obtained via the Godunov scheme is an approximation to within  $O(\Delta x^2)$  of the following Cauchy problem:

$$\begin{cases} \frac{\partial u}{\partial t} + \frac{\partial}{\partial x} f(u) = \Delta x \frac{\partial}{\partial x} \left( G(f, u, \Delta t, \Delta x) \frac{\partial u}{\partial x} \right) & t \in [t_k, t_K] \\ u(x, t_k) \text{ given.} \end{cases} \quad (12)$$

We fix the ratio  $\Delta t/\Delta x$  so that  $\Delta x$  may be treated as the parameter  $\epsilon$  in the table.

In the more general case of a system with some first-order discretization, we obtain  $W_G$  as the numerical approximation of the solution to the hyperbolic problem. Let us assume that the function  $W_G$  is the solution to

$$\begin{cases} \frac{\partial U}{\partial t} + \frac{\partial}{\partial x} F(U) = \Delta x \frac{\partial}{\partial x} \left( G_H(F, U, \Delta x, \Delta t) \frac{\partial U}{\partial x} \right) & t \in [t_k, t_K] \\ U(x, t_k) \text{ given,} \end{cases}$$

where  $G_H$  is for the numerical viscosity of the specific hyperbolic scheme with  $G_H = O(1)$ . The detection for the numerical method is based on obtaining an approximation to the residual  $\partial U/\partial t + \partial F(U)/\partial x$ .

The residual is of magnitude  $O(\Delta x^{-1})$  in either a shock layer or in a zone where a shock interacts with some other singularities. In addition, an approximation of the viscous term

$\frac{\partial^2}{\partial x^2} \bar{U}(\cdot, t_K)$  localizes some of the singularities. For example, this viscous term will be of order  $O(\Delta x^{-1})$  in a shock layer or in a zone of interaction.

Numerically it may be difficult to determine when the residual (or viscosity) is of order  $\Delta x^{-1}$ . This difficulty may usually be overcome by computing the numerical solution on two grids with different spatial spacings  $\Delta x_1$  and  $\Delta x_2$ . Let  $R_1$  and  $R_2$  be approximations to the residuals of the solutions on these meshes. When the ratio  $R_1/R_2$  of the residuals is within some tolerance of  $\Delta x_2/\Delta x_1$ , then we treat the region as being inside a shock (or shock layer). It should be mentioned that asymptotic analysis and numerical experiments show under general conditions that strong singularities are not well localized by any approximation of the gradient of the solution.

Shocks (and interactions with shocks) are easily detected and are treated in the next section. In Section 3.4, we shall show how some weak singularities that are much more difficult to localize can be absorbed in a residual correction process.

### 3.2 Numerical Treatment of Shocks

Let us first recall the numerical treatment of a simple shock for a *scalar conservation law* [1]. Let  $\Omega_0 = [a, b]$  be the zone that includes the shock (or the shock layer). First we construct an approximation  $\tilde{w}$  to the solution of (2); next, to compute an approximation to the shock location  $\tilde{S}$ , we treat the solution near the shock (or inside the shock layer).

The region  $\Omega_0$  is chosen so that  $\tilde{u}$  is an *a priori* valid approximation to  $u$  except possibly for some portion of  $\Omega_0$ ; thus,  $\tilde{w} = \tilde{u}$  outside  $\Omega_0$ . The approximation  $\tilde{w}$  is constructed inside  $\Omega_0$  with an extrapolation of  $\tilde{u}$ . This extrapolation is based on values of  $\tilde{u}$  outside  $\Omega_0$ . We construct  $\tilde{w}$  as the connection of the extrapolated values. For  $t = t_K$  fixed, we impose the area relation

$$\int_a^{\tilde{S}_K} (\tilde{w}^{left} - \tilde{u}) dx + \int_{\tilde{S}_K}^b (\tilde{u} - \tilde{w}^{right}) dx = 0$$

on the discrete problem. This is presented visually in Fig. 1, where we use second-order extrapolation and have placed  $\tilde{S}$  so that the area covered by the dark grey is equal to the area covered by the light grey. As we discuss below, the left and right values of  $\tilde{w}$  are used for the boundary conditions for the first-order approximation of the solution with a viscous profile.

Notice that the accuracy of the approximation  $\tilde{w}$  as a solution to the inviscid problem is limited only by the particular numerical techniques. Specifically, the accuracy is limited by the accuracy to which  $\tilde{u}$  is computed outside  $\Omega_0$  and by the order of accuracy of the extrapolation. There is no limitation imposed by the asymptotic analysis on this aspect of the method.

The treatment of the solution in a neighborhood of the shock (or inside the shock layer) depends on whether the goal is the solution of the viscous problem (1) or the inviscid problem (2). If the solution to inviscid problem is the goal, then we wish to minimize the viscosity. Viscous problems require the computation of the profile of the shock. The asymptotic analysis of the shock layer for a system of conservation laws is similar to the case of a scalar conservation law (cf. Section 2).

For the numeric computations, the primary difference between the treatment for a scalar conservation law and a system is that we must verify that certain conditions are satisfied by

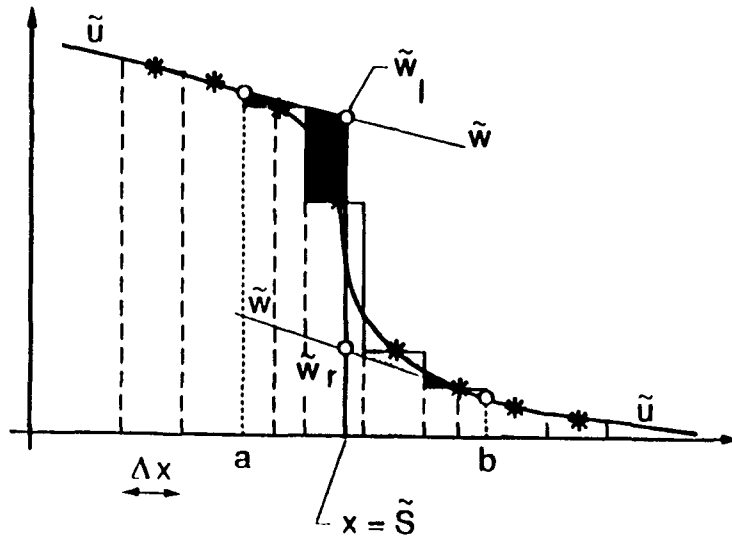


Figure 1: Approximation of shock location

the system. Specifically, we *a posteriori* (during the numerical computations) verify that

- $\tilde{W}_r^0$  and  $\tilde{W}_l^0$  are on a Rankine-Hugoniot set up to a tolerance,
- there is a trajectory from  $\tilde{W}_r^0$  to  $\tilde{W}_l^0$ , and
- $\frac{\partial \tilde{W}_{l/r}^0}{\partial \tau} = O(1)$ .

The first assumption is satisfied automatically by solutions to scalar conservation laws. Now we shall describe in more detail the numerical treatment of the shock layer depending on whether one solves an inviscid or a viscous problem.

### 3.2.1 Minimum Viscosity Method

Suppose that for a particular  $t_k$ , the shock location  $\tilde{S}$  is in  $[x_i, x_{i+1}[$ , where  $[x_i, x_{i+1}[ \subset \Omega_0$ . In the most general case,  $\tilde{S}$  will not be a grid point, and we modify  $\tilde{W}$  to maintain conservation. This step results in modifying either the value of  $\tilde{W}_i^k$  or the value of  $\tilde{W}_{i+1}^k$  (see [1] for details). The modification introduces the minimum of viscosity needed to use the Godunov method throughout the domain. This modification of  $\tilde{W}_i^k$  or  $\tilde{W}_{i+1}^k$  is the final stage of the shock layer treatment when the goal is the solution to the inviscid problem.

### 3.2.2 Viscous Problems

To solve problem (1), we implement the inner layer computation as in Section 2.2. The matching relations used to obtain a uniform approximation are based on the numerical approximation of the outer expansion. Thus, we solve (8) except that  $\tilde{W}_r^0$  and  $\tilde{W}_l^0$  are used in place of  $U_r^0$  and  $U_l^0$ , respectively.

To obtain the higher-order corrections  $\hat{U}^i$  for  $i > 0$ , we would solve the problems (9) and (10) with modified boundary conditions; however, an easy approximation can be obtained by computing a poor approximation  $\hat{U}_p^1$  to  $\hat{U}^1$  such that

$$\hat{U}^1 = \begin{cases} \bar{W} - U_l^0 & \text{for } x \leq x_j \\ \bar{W} - U_r^0 & \text{for } x \geq x_j. \end{cases}$$

The numerical treatment of this problem involves using an  $\text{ODE}^{\text{F}}$  solver to obtain the solution to the system of ODEs (8). Notice that except when the details of the viscous profiles are desired, we need only obtain the values of the inner expansion at the coarse grid points on which we know  $\bar{W}$ . Even when a higher-order numerical method is used, there are a large number of steps in the integration of the ODE system for the inner region. The cost of this integration may be reduced by using an explicit formula of approximation given by the asymptotic analysis in the neighborhood of the critical points (see [1]).

### 3.3 Interaction of Singularities

In regions where solutions to problem (1) contain shocks that interact with other singularities, we use a brute-force approach. The local scaling in both the spatial and the temporal variables is

$$\xi = \frac{x - S_0}{\epsilon}, \quad \tau = \frac{t - t_0}{\epsilon}.$$

Under this transformation the PDE that governs the solution becomes

$$\frac{\partial \tilde{U}}{\partial \tau} + \frac{\partial}{\partial \xi} F(\tilde{U}) = \frac{\partial}{\partial \xi} \left( P(\tilde{U}) \frac{\partial \tilde{U}}{\partial \xi} \right), \quad (13)$$

where  $\tilde{U}(\xi, \tau) = U(x, t)$ . This is the equation that is solved in the regions with interactions. There is no expansion of the solution used here. The transformation *a priori* resolves all of the physics. This situation is reflected by all of the terms in (13) being order unity.

The initial condition for this problem is derived by imposing  $C^0$  continuity. This was sufficient for the problems considered in this paper. However, the computation of the residual is a check of the numerical accuracy of the composite scheme. A residual correction similar to the one in the next section could be applied to improve the result. Interface boundary conditions is a topic of further study.

### 3.4 Residual Correction

Second-order accuracy in both space and time is achieved through a first-order numerical approximation followed by a residual correction. This accuracy is obtained in regions where the regular expansion (3) is valid. We also discuss the residual correction in the presence of weak singularities, where the accuracy is increased (but not as much as for the smooth regions). This discussion begins with the asymptotic analysis, is followed by the choice of the particular discretization, and ends with the treatment of weak singularities.

### 3.4.1 Asymptotic Analysis

The asymptotic analysis is based on the regular expansion presented in Section 2.1. Thus, this analysis is restricted to regions where the solution is smooth and the regular expansion is valid. For convenience, our analysis assumes  $\epsilon$  and  $\Delta t$  are both  $O(\Delta x)$ . The dependency of  $\epsilon$  on  $\Delta x$  is related to the order of the regular expansion and the hyperbolic scheme used.

The Godunov method applied to (2) gives us  $W_G$  as a first approximation to the solution to the parabolic problem (1); thus  $U = W_G + O(\Delta t, \Delta x)$ . A single correction  $W_c$  will be computed so that

$$U = W_G + hW_c + h^2W_2 + O(h^3), \quad (14)$$

where  $h$  is a small parameter of magnitude  $O(\Delta t) = O(\Delta x)$ . The equation for  $W_c$  is determined with an analysis similar to that of the regular expansion.

The viscous terms now arise from both the viscosity in (1) and from the numerical error in  $W_G$ , resulting in the linear problem

$$\begin{cases} \frac{\partial W_c}{\partial t} + \frac{\partial}{\partial x}(DF(U)W_c) = R(W_G) \\ W_c(x, 0) = 0 \end{cases} \quad (15)$$

for  $W_c$ . Here,

$$hR(W_G) = \nu \frac{\partial}{\partial x} \left( P(W_G) \frac{\partial W_G}{\partial x} \right) - \left( \frac{\partial W_G}{\partial t} + \frac{\partial}{\partial x} F(W_G) \right), \quad (16)$$

where  $\nu = \epsilon$  or  $\nu = 0$ , depending on whether we are solving the viscous problem or the inviscid problem. Notice that the terms of higher order would be included in the next term of the regular expansion of  $U$ . The right-hand side in the equation of (16) is the residual from using  $W_G$  as an approximation to the solution of (1). To obtain a second-order method, we start with the first-order approximation  $W_G$ , then compute the right-hand side of (16) to second-order accuracy, and finish with a first-order scheme for (15).

The asymptotic techniques are similar in the more general case when  $\epsilon$  is not of size  $O(\Delta x)$ , and/or when a different order method is used to compute  $W_G$ . Consider the case when the numerical method is  $O(\Delta x^p, \Delta t^q)$ . In this case we choose the parameter  $h$  in the expansion (14) to have magnitude equal to the largest of  $\Delta x^p$ ,  $\Delta t^q$ , and  $\nu$ . The problems for the terms in the regular expansion are obtained by identification in  $h$  after substitution of the expansion into

$$\frac{\partial U}{\partial t} + \frac{\partial}{\partial x} F(U) = \nu \frac{\partial}{\partial x} \left( P(U) \cdot \frac{\partial U}{\partial x} \right) + \Delta x^p P_1(U) + \Delta t^q P_2(U),$$

where  $\nu = 0$  or  $\epsilon$ , and  $P_1$  and  $P_2$  are terms of  $O(1)$ . We do not require specific forms for  $P_1$  and  $P_2$  for the numerical method since we may use a residual in place of  $\Delta x^p P_1(U) + \Delta t^q P_2(U)$ .

### 3.4.2 Discretization of Correction

Here, we choose discretizations for the numerical approximation of the residual and the correction scheme. Notice that these discretizations as well as the choice of the Godunov method for the first approximation are only examples of possible treatments.

Centered differences are used throughout this section; hence, the resulting finite-difference scheme will be a conservative discretization.

**Residual.** Here we use the discretization based on centered differences and averaging. The temporal derivative is approximated by  $\partial W_G(x_i, t_{k+1/2})/\partial t \approx \delta_t W_{G,i}^{k+1/2}$ , where we use the notation  $\delta$  to be the centered difference operator

$$\delta_{2\eta}g(\eta) = \frac{g(\eta + \Delta\eta) - g(\eta - \Delta\eta)}{2\Delta\eta}.$$

The formula for the complete residual is

$$R_i^{k+1/2} = \frac{1}{h} \left\{ - \left[ \delta_t W_{G,i}^{k+1/2} + \frac{1}{2} \left( \delta_{2x} F_i^{k+1} + \delta_{2x} F_i^k \right) \right] \right. \\ \left. + \frac{\nu}{2} \left[ \delta_x (P_i^k \delta_x W_{G,i}^k) + \delta_x (P_i^{k+1} \delta_x W_{G,i}^{k+1}) \right] \right\}. \quad (17)$$

Here we use the notation  $F_i^k = F(W_{G,i}^k)$  and the average  $P_{i+1/2}^k = (P(W_{G,i}^k) + P(W_{G,i+1}^k))/2$ . Taylor series analysis can be used to verify that this is an  $O(\Delta x^2, \Delta t^2)$  approximation to the residual at the point  $(x, t) = (x_i, t_{k+1/2})$ .

**Correction Scheme.** The implicit scheme based on a centered spatial derivative and a centered temporal derivative is used for the discretization of  $W_c$  to obtain

$$\delta_t W_{c,i}^{k+1/2} + \delta_{2x} \left( DF(W_{G,i}^{k+1}) \cdot W_{c,i}^{k+1} \right) = \frac{1}{h} R_i^{k+1/2}. \quad (18)$$

This is a first-order accurate method.

The accuracy of the discretization for the residual is balanced with the accuracy of the discretization for the correction term. We compute  $W_G$  to first order. The residual is computed to second order; however, it is scaled by  $1/h$  for the computation of the correction. This results in a first-order approximation to the source term for the correction. The correction discretization is first order; hence the overall method is second order.

### 3.4.3 Weak Singularities

A modification of the above analysis can be used to develop the residual correction in the presence of weak singularities because the residual is still small in the neighborhood of a weak singularity (cf. Table 1). The numerical algorithm is the same for this case; however, the analysis (and resulting accuracy) are different. In place of (14) we have the regular asymptotic expansion

$$U = W_G + \hat{W}_1 + \dots,$$

where  $W_G$  is the approximation of  $U$  obtained from the numerical method. The function  $W_G$  is an approximation to the solution of

$$\frac{\partial U}{\partial t} + \frac{\partial}{\partial x} F(U) = \nu \frac{\partial}{\partial x} \left( G(U) \frac{\partial U}{\partial x} \right),$$

where  $\nu = \epsilon$  or  $\nu = 0$ . However,  $W_G$  may be treated as the exact solution of the modified equation

$$\frac{\partial W_G}{\partial t} + \frac{\partial}{\partial x} F(W_G) = \hat{h} \text{ RHS}, \quad (19)$$

where  $\hat{h} = o(1)$  is defined such that  $RHS = O_s(1)$  is true *a priori*. So we rescale  $\hat{W}_1$  as:  $\hat{W}_1 = \hat{h}\hat{W}_c$ . As in Section 3.4.1, we obtain the equation for  $\hat{W}_c$  as

$$\frac{\partial \hat{W}_c}{\partial t} + \frac{\partial}{\partial x}(DF(W_G) \cdot \hat{W}_c) = -RHS + \frac{\nu}{\hat{h}} \frac{\partial}{\partial x} \left( G(W_G) \frac{\partial W_G}{\partial x} \right).$$

This is the equation for the correction term in the presence of weak singularities.

The numerical discretizations used for the case of the weak singularity can be the same as those presented in the last section. For example, when the singularity is of order  $\hat{h} = O(\sqrt{\epsilon})$ , then the method with the same discretizations will have accuracy  $O(\hat{h}^2) = O(\epsilon)$ . Both forms of the analysis in this section are valid with the numerical discretizations of the previous two sections. The numerical method after the residual correction will be more accurate than using the first approximation  $W_G$  alone. In addition, it is feasible to use a higher-order method for the discretizations of the residual and a higher-order expansion for the correction in regions of weak singularities.

### 3.5 Numerical Algorithm

The numerical and asymptotic analysis are combined and summarized in Algorithm 1 below. The outer region is discretized by using the coarsest grid. Numerical values of  $W_G$  and  $W_c$  are determined at coarse grid points.  $W_G$  is computed over the whole grid; however, the coarse grid values located inside refined regions are used only in the conservation relation. The refined grid values are injected into these coarse grid values at the end of the time step. Linear interpolation is used to obtain values of the coarse grid solution between points when necessary.

The numerical results presented here involve only a two-level refinement. This is because the current implementation is designed for problems in which shocks (or shock layers) and their interactions are the only strong singularities. We recall that weak singularities are treated by the residual correction scheme.

The numerical solution in the shock layer is computed in the transformed coordinates (5) when the shock profile is not rapidly varying. When interactions exist, the coordinates use the same  $\xi$  with the temporal scaling  $\tau = t/\epsilon$ . Although  $\Delta\xi$  is the same magnitude as  $\Delta x$ , local spatial scaling is used. This means that a region of size  $\Delta x$  in the coarse grid corresponds to many points in the  $\xi$ -grid. For this reason, we refer to the  $\xi$ -grid as the refined grid.

The method is adaptive. The refined grid is allowed to change shape and location as the solution evolves. The refined region contains an overlap region where both the inner and outer solutions are valid.

## 4 Experiments

In this section we demonstrate the techniques developed within this paper. The experiment in Section 4.1 demonstrates the residual correction. The experiments in Section 4.2 demonstrate the method on the isentropic gas dynamic equations.

For  $k = 1, \dots$

- I. March from  $t_k$  to  $t_{k+1}$  on two coarse meshes with spatial discretizations  $\Delta x_1 \neq \Delta x_2$ .
- II. Detection.
  - A. On each coarse mesh compute the residual used in Table 1. (Alternatively, compute the viscosity.)
  - B. Mark regions that should be refined.
- III. Compute  $W_C$  with the residuals of Step II.A. except in marked regions.
  - A. Modify the shape of the refined region.
- IV. March the marked regions from  $t_k$  to  $t_{k+1}$  according to the type of singularity.
  - A. For a simple shock of Section 2.3, compute the solution to the ODEs as outlined in that section.
  - B. For an interaction of singularities of Section 3.3:
    1. Form the initial condition in newly refined regions.
    2. Determine boundary conditions from linear interpolation.
    3. March inner solution  $\Delta t / (\epsilon \Delta \tau)$  time steps.
- V. Inject the values from the internal layer to obtain the composite uniform approximation.

ALGORITHM 1 *Numerical algorithm*



## 4.1 Solving Burgers' Equation

The residual correction technique is demonstrated by solving the inviscid Burgers' equation

$$\frac{\partial u}{\partial t} + u \frac{\partial u}{\partial x} = 0$$

on the domain  $[-0.2, 1]$  with a wedge initial condition. The first approximation is obtained with a first-order Godunov method using discretization parameters  $\Delta x = .025$  and  $\Delta t = .0125$ . The solution at time  $t = .5$  is presented in Fig. 2. The increase in accuracy of

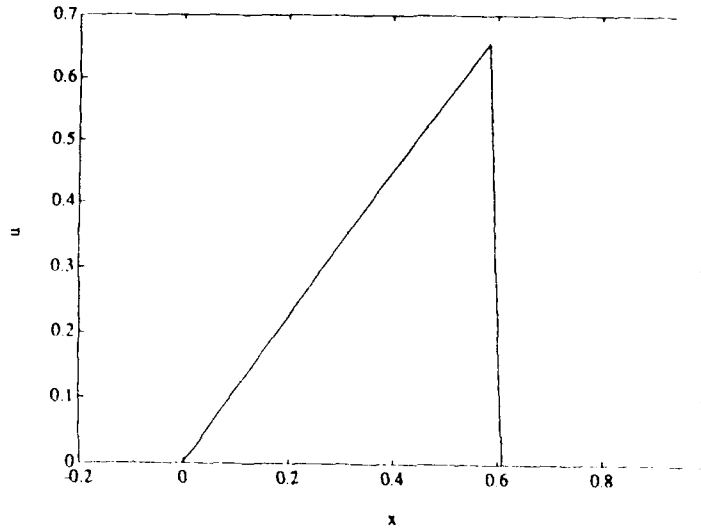


Figure 2: Exact solution to Burgers' equation

the residual correction over using just the Godunov is shown in Figs. 3-4. The minimum viscosity method is used for the numerical solution in a neighborhood of the shock. A cutoff function is used for the residual correction. This causes the correction to be applied only outside a neighborhood of the shock. The mass that might be lost or gained in this procedure is included in the computations for the minimum viscosity method. The large jump at the shock is a reflection of the error between the  $L_2$  projection of the numerical solution with the exact solution.

## 4.2 Solving the Isentropic Gas Dynamic Equations

In this section the method is demonstrated on the system

$$\frac{\partial u}{\partial t} - \frac{\partial v}{\partial x} = 0$$
$$\frac{\partial v}{\partial t} + \frac{\partial}{\partial x} \left( \frac{1}{u^\gamma} \right) = \epsilon \frac{\partial}{\partial x} \left( \frac{\partial u}{\partial x} \right).$$

Here  $u$  is the inverse of the density and  $v$  is the velocity. These equations are obtained from the conservation of mass and momentum in Lagrangian coordinates assuming that  $u$

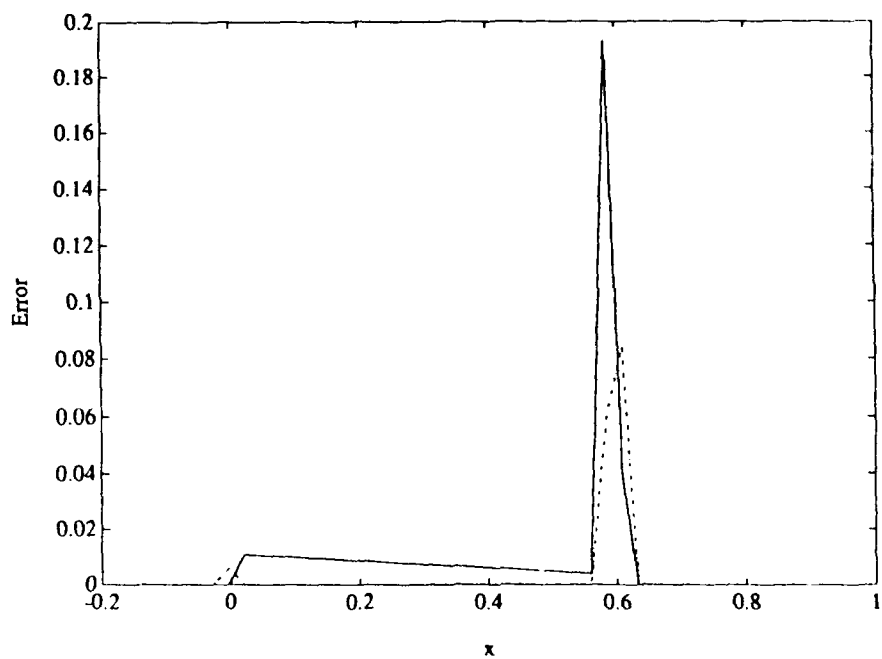


Figure 3: Error in whole domain with (dashed) and without (solid) residual correction

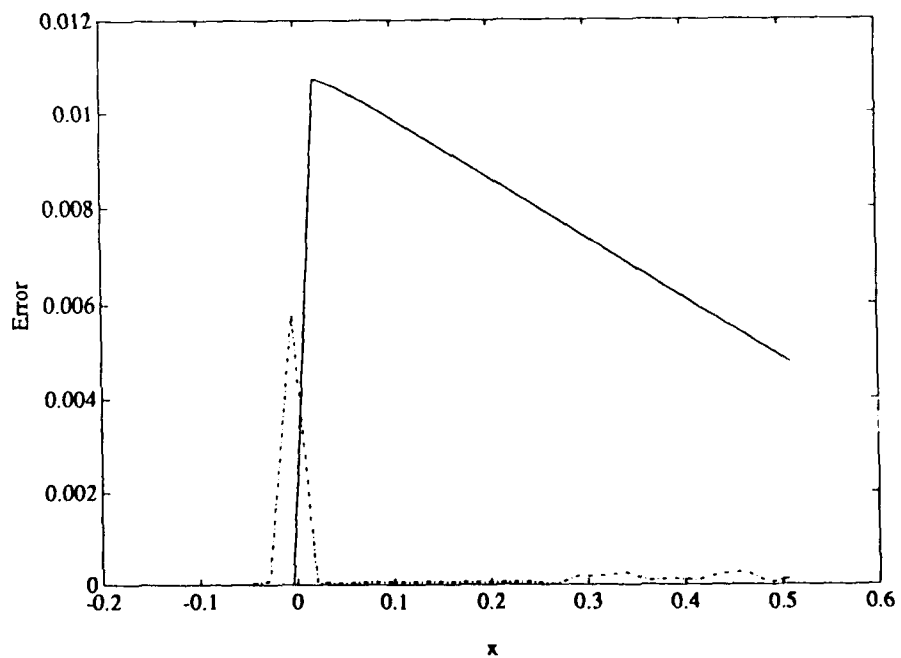


Figure 4: Error in corner-layer region with (dashed) and without (solid) residual correction

is equal to the pressure raised to the  $-1/\gamma$ th power (the perfect gas law) with  $\gamma = 2.2$ . The numerical solution in the outer region is computed with a first-order Godunov method with CFL number  $\Delta t/\Delta x = .2$ . The discretization on the scaled coordinates inside the shock layer is based on  $\Delta \xi = .1$ . We use a third-order Runge Kutta method to compute the viscous profile for a shock layer. To compute a parabolic layer, we use an explicit first-order ENO scheme (similar to the Godunov scheme) with the CFL condition  $\Delta \tau/\Delta \xi \leq .2$  and stability condition  $\Delta \tau/\Delta \xi^2 \leq .25$ . These values are within the limits imposed for the stability of the finite difference method.

#### 4.2.1 Simple Shock

The first experiment is a simple shock. In Fig. 5 we show the computed solution using various methods. The initial condition is

$$u(x, 0) = \begin{cases} U_L, & \text{for } x < 0 \\ U_R, & \text{for } x \geq 0 \end{cases} \quad (20)$$

$$v(x, 0) = \begin{cases} V_L, & \text{for } x < 0 \\ V_R, & \text{for } x \geq 0 \end{cases} \quad (21)$$

where

$$U_R = 2.50, \quad U_L = .800, \quad V_R = .600,$$

$$\text{and } V_L = V_R + \sqrt{-\left(\frac{1}{U_R^\gamma} - \frac{1}{U_L^\gamma}\right)(U_R - U_L)}$$

The value for  $V_L$  is chosen using the Rankine-Hugoniot condition

$$\frac{V_L - V_R}{U_R - U_L} = \frac{1/U_R^\gamma - 1/U_L^\gamma}{V_R - V_L}.$$

The computations are run with  $\Delta x = .02$ . The Godunov and minimum viscosity methods approximate the solution to the hyperbolic problem, whereas the ODE layer (solving problem (8) inside the shock layer) and the parabolic-layer methods are used to compute the numerical approximation to the viscous problem with  $\epsilon = .01$ .

The minimum viscosity method introduces significantly less viscosity than the Godunov method. As expected, the parabolic-layer and the ODE-layer methods produce numerical solutions that are very close to each other.

#### 4.2.2 Shock-Rarefaction Interaction

The method was also used to solve a Riemann problem with a right-traveling shock and a left-propagating rarefaction. Thus, for the small time, we must solve an initial layer with a shock-rarefaction interaction. We can compute the exact solution of the inviscid problem. First, an analytic self-similar solution (a rarefaction emanating from the origin) to the inviscid isentropic gas dynamic equations is given by

$$u(x, t) = \gamma^{1/(\gamma+1)} \left(\frac{x}{t}\right)^{-2/(\gamma+1)} \quad (22)$$

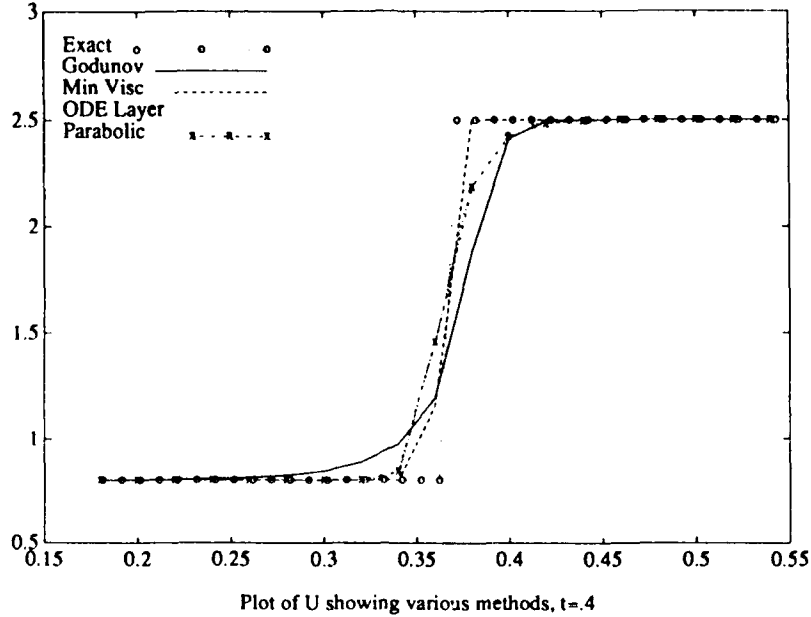


Figure 5: Numerical solutions to the isentropic system,  $t = .4$

$$v(x, t) = \frac{2\gamma^{1/(\gamma+1)}}{\gamma - 1} \left(\frac{x}{t}\right)^{\frac{\gamma-1}{\gamma+1}} + const. \quad (23)$$

An initial condition with a shock and rarefaction emanating from the origin is constructed by connecting left values  $(U_L, V_L)$  to middle values  $(U_o, V_o)$  with a rarefaction. The middle values are connected to the right values  $(U_r, V_r)$  with a shock. In our experiment the initial condition is given by (20),(21) where

$$U_L = 1.4709, \quad U_R = 2.5000, \quad V_L = 1.0388, \quad V_R = 0.8050.$$

The middle value of the solution between the shock and rarefaction is  $(U_o, V_o) = (1.973, 1.356)$ . We expect the viscous perturbation to have little or no effect on the speed at which shocks and rarefactions travel; thus, we shall compare the viscous solutions to the exact solution of the inviscid problem given above.

In Fig. 6 the exact solution to the inviscid problem is compared with the computed solution, where  $\Delta x = .02$  and  $\epsilon = .01$ . This plot shows that the shock speed and rarefaction propagation are nearly the same for both solutions. Greater detail is shown for the shock layer in Fig. 7. Here we use  $\delta_x = 2\epsilon$ . This plot demonstrates that the method has the correct shock speed and that the solutions are converging to the inviscid solution as  $\epsilon \downarrow 0$ . Detail of the rarefaction for the same runs is shown in Fig. 8. Here the offset to the location of the rarefaction is  $\Delta x/2$  and can be attributed to the initial condition for the parabolic layer.

This is a domain decomposition method. The internal-layer domain is detected by comparing the second derivate to tolerance of  $const\epsilon$ . The jump in internal-layer subdomain boundary as depicted in Fig. 9 is caused by the steady smoothing of the rarefaction until it is no longer detected by the residual or second derivative test. Also for  $t \geq 0.2$  a simple shock is detected and can be solved by the ODE layer method.

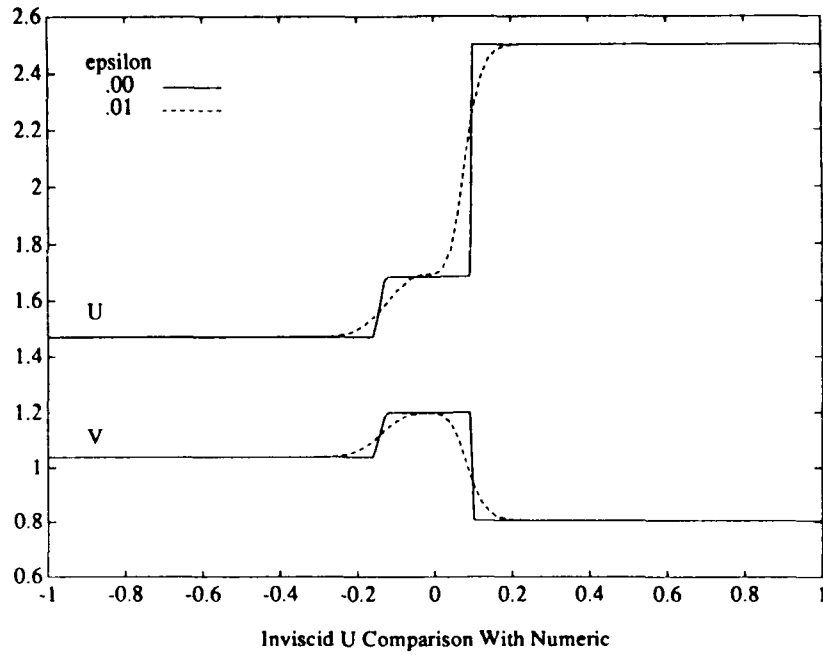


Figure 6: Viscous numeric compared with inviscid exact,  $t = .2$

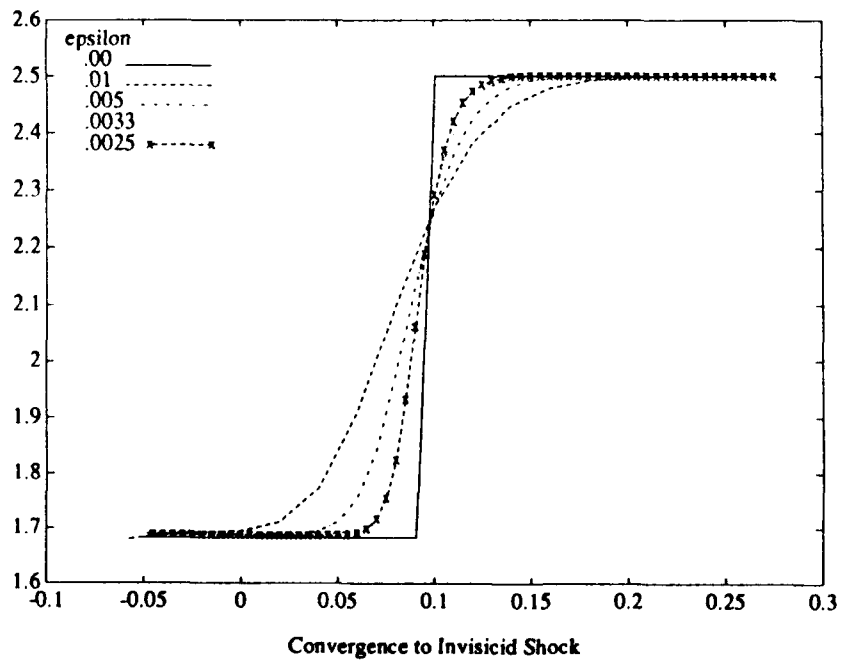


Figure 7: Viscous numeric compared with inviscid exact,  $t = .2$ .

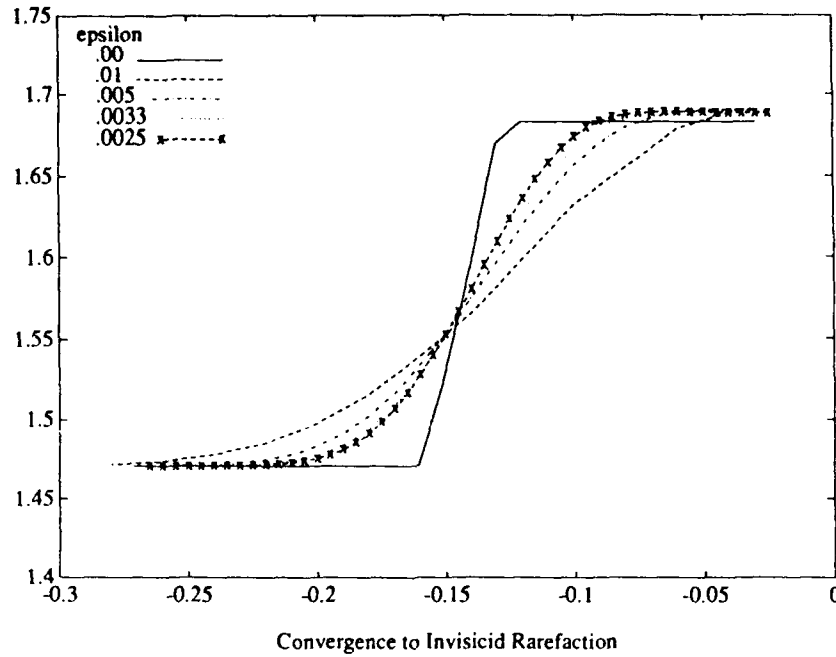


Figure 8: Viscous numeric compared with inviscid exact,  $t = .2$ .

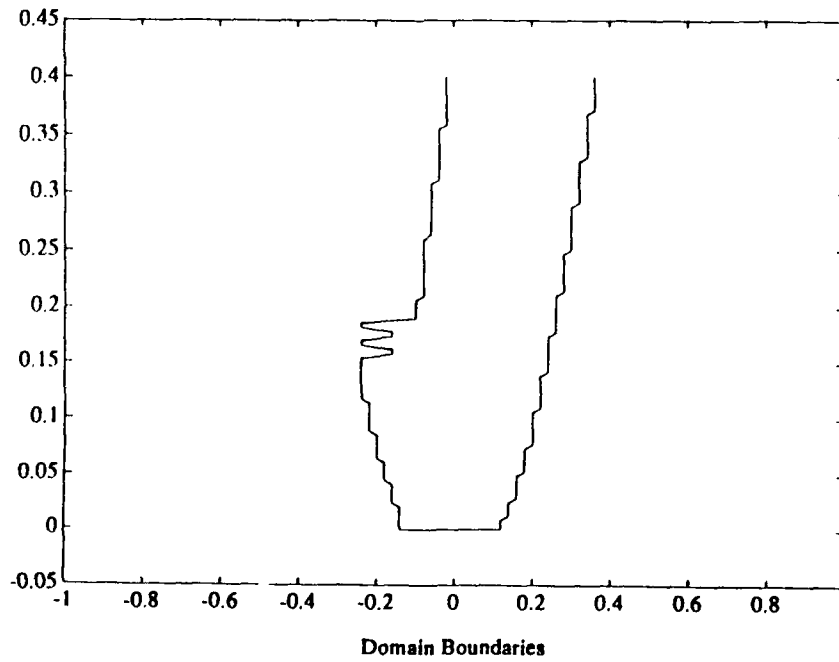


Figure 9: Internal-layer subdomain for a shock-rarefaction interaction.

## References

- [1] A. Bourgeat and M. Garbey, *Computation of viscous (or nonviscous) conservation law by domain decomposition based on asymptotic analysis*, Preprint 86, equipe d'analyse numerique, LYON-St Etienne, September 1989.
- [2] R. C. Y. Chin, G. W. Hedstrom, J. R. McGraw, and F. A. Howes, *Parallel computation of multiple-scale problems*, in *New Computing Environments: Parallel, Vector, and Systolic*, A. Wouk, ed., SIAM, Philadelphia, 1986, pp. 136-153.
- [3] R. C. Y. Chin and R. Krasny, *A hybrid asymptotic-finite element method for stiff two-point boundary value problems*, SIAM J. Sci. Stat. Comp. **4** (1983), 229-243.
- [4] C. C. Conley and J. A. Smoller, *Shock waves as limits of progressive wave solutions of higher order equations*, Comm. Pure Appl. Math **24** (1971), 459-472, and Comm. Pure Appl. Math **25** (1972), 133-146.
- [5] W. Eckhaus, *Asymptotic Analysis of Singular Perturbations*, North-Holland, Amsterdam, 1979.
- [6] P. C. Fife, *Dynamics of internal layers and diffusion interfaces*, in SIAM Regional Conference, *Series in Applied Mathematics*, SIAM, Philadelphia, 1988.
- [7] M. Garbey, *Quasilinear hyperbolic-hyperbolic singular perturbation problem: Study of a shock layer*, Mathematical Methods in the Applied Sciences **11** (1989), 237-252.
- [8] M. Garbey, *Asymptotic analysis of singular perturbation problems governed by a conservation law*, Preprint MCS-P107-1089, MCS, Argonne National Laboratory, October 1989.
- [9] M. Garbey, *Singular perturbation problem governed by system of conservation laws*, MCS-P172-0890
- [10] F. A. Howes, *Multi-dimensional initial-boundary value problems with strong nonlinearities*, Arch. for Rat. Mech. Anal. **91** (1986), 153-168.
- [11] P. D. Lax, *Hyperbolic Systems of Conservation Laws and the Mathematical Theory of Shock Waves*, SIAM, Philadelphia, 1973.
- [12] T. P. Liu, *The entropy condition and the admissibility of shocks*, J. Math. Anal. and Appl. **53** (1976), 78-88.
- [13] T. Nishida, *Global solution for initial boundary value problem of a quasi linear hyperbolic system*, Proc. Jap. Ac. **44** (1968), 642-646.
- [14] O. Oleinik, *Discontinuous solutions of nonlinear differential equations*, American Mathematics Society Translations (1976), 95-172.

- [15] J. S. Scroggs and D. C. Sorensen, *An asymptotic induced numerical method for the convection-diffusion-reaction equation*, in *Mathematics for Large Scale Computing*, J. Diaz, ed., Marcel Dekker, New York, 1989, pp. 81-114.





# Report Documentation Page

1. Report No. NASA CR-187483 ICASE Report No. 90-87	2. Government Accession No.	3. Recipient's Catalog No.	
4. Title and Subtitle  ASYMPTOTIC-INDUCED NUMERICAL METHODS FOR CONSERVATION LAWS	5. Report Date  December 1990	6. Performing Organization Code	
	7. Author(s) Marc Garbey Jeffrey S. Scroggs	8. Performing Organization Report No.  90-87	
9. Performing Organization Name and Address Institute for Computer Applications in Science and Engineering Mail Stop 132C, NASA Langley Research Center Hampton, VA 23665-5225	10. Work Unit No.  505-90-21-01	11. Contract or Grant No.  NAS1-18605	
	12. Sponsoring Agency Name and Address National Aeronautics and Space Administration Langley Research Center Hampton, VA 23665-5225	13. Type of Report and Period Covered  Contractor Report	14. Sponsoring Agency Code
15. Supplementary Notes Langley Technical Monitor: Richard W. Barnwell Proceedings of Asymptotic Analysis and Numerical Solution of Partial Differential Equations  Final Report			
16. Abstract  Asymptotic-induced methods are presented for the numerical solution of hyperbolic conservation laws with or without viscosity. The methods consist of multiple stages. The first stage is to obtain a first approximation by using a first-order method, such as the Godunov scheme. Subsequent stages of the method involve solving internal-layer problems identified by using techniques derived via asymptotics. Finally, a residual correction increases the accuracy of the scheme. The method is derived and justified with singular perturbation techniques.			
17. Key Words (Suggested by Author(s)) domain decomposition, singular perturbations, asymptotics	18. Distribution Statement 34 - Fluid Mechanics and Heat Transfer 64 - Numerical Analysis  Unclassified - Unlimited		
19. Security Classif. (of this report) Unclassified	20. Security Classif. (of this page) Unclassified	21. No. of pages 24	22. Price A03